Advanced Materials Research Vol. 1053 (2014) pp 343-350
Online available since 2014/Oct/20 at www.scientific.net
© (2014) Trans Tech Publications, Switzerland
doi:10.4028/www.scientific.net/AMR.1053.343

Submitted: 21.07.2014
Accepted: 28.07.2014

Multifractal, Structural and Optical Properties of HfO_2 Thin Films

LI Zhi[1,a], MA Chun-yu[2,b], ZHANG Qing-yu[2,c]

[1.] Department of Mechanical Engineering, Dalian University, Dalian 116622, China;

[2.] Key Laboratory of Materials Modification by Laser, Ion and Electron beams, (Dalian University of Technology), Ministry of Education, Dalian 116024, China;

[a]lizhi@dlu.edu.cn; [b]chunyuma@dlut.edu.cn; [c]qyzhang@dlut.edu.cn;

Keywords: hafnium dioxide; substrate temperature; structural; multifractal analysis

Abstract. HfO_2 films were sputter deposited under varying substrate temperatures (T_s) and their structural and morphological characteristics, optical properties were systematically studied by means of X-ray diffraction (XRD), atomic force microscope (AFM), and UV/VIS spectrophotometry. A statistical analysis based on multifractal formalism shows the uniformity of the height distribution increases as T_s is increased and the widths $\Delta\alpha$ of multifractal spetra are related to the average grain size $D_{(-111)}$ as $\Delta\alpha \sim [D_{(-111)}]^{-0.83}$. The monoclinic HfO_2 is highly oriented along (-111) direction with increasing T_s. The Lattice expansion increases with diminishing HfO_2 crystalline size below 7 nm while maximum lattice expansion occurs with highly oriented monoclinic HfO_2 of crystalline size about 14.8 nm. The film growth process at $T_s \geq 200^{o}$C with surface diffusion energy of ~ 0.29 eV is evident from the structural analysis of HfO_2 films.

Introduction

Hafnium dioxide (HfO_2) is a wide band gap, high dielectric constant, and high refractive index insulator with good thermal stability. On the basis of these properties, thin film HfO_2 has been investigated for use in the field of electronics, magnetoelectronics, structural ceramics, and optoelectronics [1, 2]. HfO_2 has been identified as one of the most promising materials for high-*k* replacement of SiO_2 in the next generation complementary metal-oxide-semiconductor devices [3]. These interesting applications have led to numerous efforts to synthesize HfO_2 films by various techniques, including chemical vapor deposition (CVD)[4], sol-gel process[5], pulsed laser deposition[6], electron beam evaporation and sputtering[7,8], among them, reactive sputtering being one of the most widely used.

In sputtering technique, controlled growth and manipulation of structures at the nanoscale dimensions has important implications for the applications of HfO_2. However, it is well known that the film's optical and electronic properties are highly dependent on the structural characteristics (i.e., structure, crystallite size, crystallographic texture and morphology) and chemistry, which in turn controlled by the fabrication technique, growth conditions etc. From the viewpoint, the ability to tailor the properties so as to optimize performance requires detailed understanding of the structural characteristics of HfO_2 films. In this study, the influence of growth temperature on the structural characteristics of rf sputtered HfO_2 films has been investigated. The surface morphologies of HfO_2 films grown at various temperatures were measured by atomic force microscope (AFM). The multifractal spectra f (α) have been used to characterize the AFM images.

The concept of multifractal measure was first introduced by Mandelbrot [9] in order to study several features in the intermittency of turbulence. The multifractality and its formalism were further developed by many other authors and applied in several fields of the science: biology [10], geology [11], physics [12-13], etc. Since Fractal dimensions values are sensitive to the combined effects of morphology, crystal size and the spatial distribution of grain within the film, the morphological features of the surfaces can be described by a fractal model quantitatively. By using the multifractal approach can get more detailed information than the simple fractal. Raoufi *et al* [14] have shown the nonuniformity of the height distribution for ITO thin films increases with the increasing annealing temperature by use of the multifractal analysis. Chen *et al.* [15] have studied the relationship between the dimension and the distribution of fractal patterns in annealed Au/Ge bilayer films. They found that the fractal crystallization process in the films can be characterized by the multifractal approach. We developed the multifractality and its formalism to investigate the surface morphologies of HfO_2 films grown at various temperatures by rf reactive sputtering from their atomic force microscopy (AFM) images.

Experimental details

HfO_2 films were deposited on both fused SiO_2 substrates and *n*-type-doped Si (001) wafers by reactive rf magnetron sputtering from a metallic hafnium (Hf) target with a diameter of 60 mm. The vacuum chamber was evacuated to 8.5×10^{-4} Pa using a turbomolecular pump. The used sputtering gas (Ar) and the reactive gas (O_2) were 99.999% pure and introduced into chamber by separate inlets and controlled by standard mass flow controllers. Deposition was carried out at 0.5 Pa in ambient mixtures of Ar at 30 SCCM (standard-state cubic centimeter minute) and O_2 at 5 SCCM. The power applied to the target was 120 W. The distance between the target and the substrate was 70mm. The samples were deposited for 2 hours at substrate temperature of RT (28-47 °C), 200 °C, 400 °C, 600 °C, respectively. The crystallographic orientation of the films was investigated by x-ray diffraction (XRD) using Cu $K\alpha$ radiation. The measurement of transmittance (*T*) and reflectance (*R*) at normal incidence of the films were performed using a Lambda-35 UV/VIS spectrometer. Atomic force microscopy (AFM) on a CSPM5500 scanning probe microscope was used in contact mode to measure the surface morphologies of the films.

Multifractal spectra of AFM images are calculated by box-counting method. The images can be divided into many boxes of size $l\times l$ ($\varepsilon=l/L$, L=512). We use the following definition of measure:

$$P_{ij}(\varepsilon)=\frac{h_{ij}}{\sum h_{ij}} \tag{1}$$

where $P_{ij}(\varepsilon)$ is the average deposition probability of the film in the box (i,j). h_{ij} is the average height of the box (i,j) of size ε measured from the datum planes having the same depth for the substrate and the HfO_2 thin film deposits. $P_{ij}(\varepsilon)$ can be described as mutifractal as

$$P_{ij}(\varepsilon)\sim\varepsilon^{\alpha} \tag{2}$$

$$N_{\alpha}(\varepsilon)\sim\varepsilon^{-f(\alpha)} \tag{3}$$

where α is the singularity of the subset of probabilities, $N_{\alpha}(\varepsilon)$ is the number of boxes where the probability has singularity between α and α+dα, and $f(\alpha)$ is the fractal dimension of the set of boxes with singularity α. The partition function $Z(q,\varepsilon)$ used for multifractal analysis is a two variables function. It is defined and expressed as a power law of ε with an exponent $\tau(q)$, where q is the moment order:

$$Z(q,\varepsilon)=\sum P_{ij}^{q}(\varepsilon)=\varepsilon^{\tau(q)} \tag{4}$$

The fractal dimension f (α) can be obtained by performing the Legendre transformation as follows:

$$\alpha = \frac{d[\tau(q)]}{dq} \tag{5}$$

$$f(\alpha) = \alpha q - \tau(q) \tag{6}$$

The width of the multifractal spectrum is $\Delta\alpha$ and the difference of the fractal dimensions of the maximum probability subset ($\alpha = \alpha_{min}$) and the minimum one ($\alpha = \alpha_{max}$) is Δf ($\Delta f = f(\alpha_{\min}) - f(\alpha_{\max})$).

Results and discussion

Surface morphology and multifractal analysis. Fig.1 shows large-scale (2×2 μm^2) AFM images of HfO_2 thin films grown at RT, 200 °C, 400 °C and 600 °C, respectively. There are two patterns seen in the lumps. The first is where the surface height (peak to valley) decreases with increased substrate temperature. The second is where the lateral size of the film grown at 600 °C is markedly smaller than that of the films grown at temperatures from RT to 400 °C. The results (R_a and rms) have been listed in Table 1. It can be see that the average roughness R_a and rms values decreased as substrate temperature is increased.

We calculated the partition function $\boldsymbol{Z}(q,\varepsilon)$ for q ranging from -10 to 10 with a step of 0.5. Fig.2(a) shows ln $\boldsymbol{Z}(q,\varepsilon)$ - ln ε curves obtained from AFM images of HfO_2 films grown at RT. Regular multifractal behavior has strict linearity in the ln $\boldsymbol{Z}(q,\varepsilon)$ - ln ε plot for all moments of q and this linearity can approach zero infinitely (ln $\varepsilon \to -\infty$). In our calculations, the height corresponds to the local growth probability and can be obtained from Eq. (1). The box sizes ε are taken as 1/512, 1/256, 1/128, 1/64, 1/32, 1/16, 1/8, 1/4, 1/2 and 1. It can be seen that the linearity of ln $\boldsymbol{Z}(q,\varepsilon)$ - ln ε curves is excellent at all q moments. The ln $\boldsymbol{Z}(q,\varepsilon)$ versus ln ε curves of HfO_2 films grown at other temperatures can be obtained by the same method (no showing here). Consequently, the multifractal analysis was used to characterize the AFM images of HfO_2 films quantitatively.

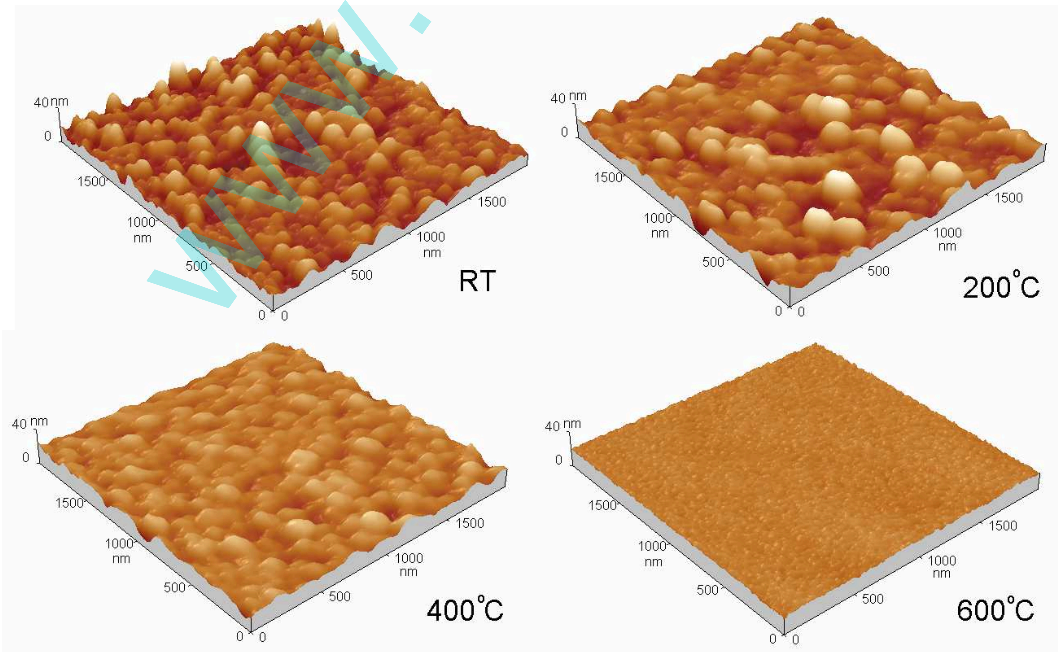

Fig.1 AFM images of HfO_2 films grown at various temperatures

Fig. 2(b) shows the multifractal spectra $f(\alpha)$ of the samples. The parameters of the multifractal spectra are summarized in Table 1. It can be seen that the shape and the spectrum width ($\Delta\alpha = \alpha_{max} - \alpha_{min}$) of the $f(\alpha)$ are different. It can be seen that the $\Delta\alpha$ decreases as the increasing substrate temperature, indicating the height probability becomes more uniform. Since $\varepsilon < 1$, α_{min} presents the maximum probability ($P_{max} \sim \varepsilon^{\alpha min}$) and α_{max} the minmum one ($P_{min} \sim \varepsilon^{\alpha max}$). Therefore, the $\Delta\alpha$ can be used to describe the range of the probability due to $P_{max}/P_{min} \sim \varepsilon^{-\Delta\alpha}$. One exists that the smaller the $\Delta\alpha$, the narrower the probability distribution, and the smaller the difference between the highest and the lowest growth probability. We found that the Δf of the multifractal spetra of the HfO_2 films is all bigger than zero. Due to the $f(\alpha_{min})$ represents the number of the boxes of the same maximum height probability ($N_{P\max}(\varepsilon) = N_{\alpha\min}(\varepsilon) \sim \varepsilon^{-f(\alpha min)}$), while $f(\alpha_{max})$ reflects the number of the minimum one ($N_{P\min}(\varepsilon) = N_{\alpha\max}(\varepsilon) \sim \varepsilon^{-f(\alpha max)}$), the Δf describes the ratio of the number of the maximum probability and that of the minimum one: $N_{P\max}(\varepsilon)/N_{P\min}(\varepsilon) = \varepsilon^{-\Delta f}$. Thus, $\Delta f > 0$ means that the chance of the height distribution of the deposit lying at highest sites is more than that at lowest sites ($N_{H\max}/N_{H\min} > 1$) and vice versa. Experimental results indicate that the number of lowest valleys of all HfO_2 films is larger than that of the highest peaks (at $\varepsilon = 1/512$, $N_{H\max}/N_{H\min} \approx$ 3, 77, 11, 29 for HfO_2 grown at RT, 200 °C, 400 °C and 600 °C, respectively). Note that, the conventional statistical treatments cannot give this quantitative description.

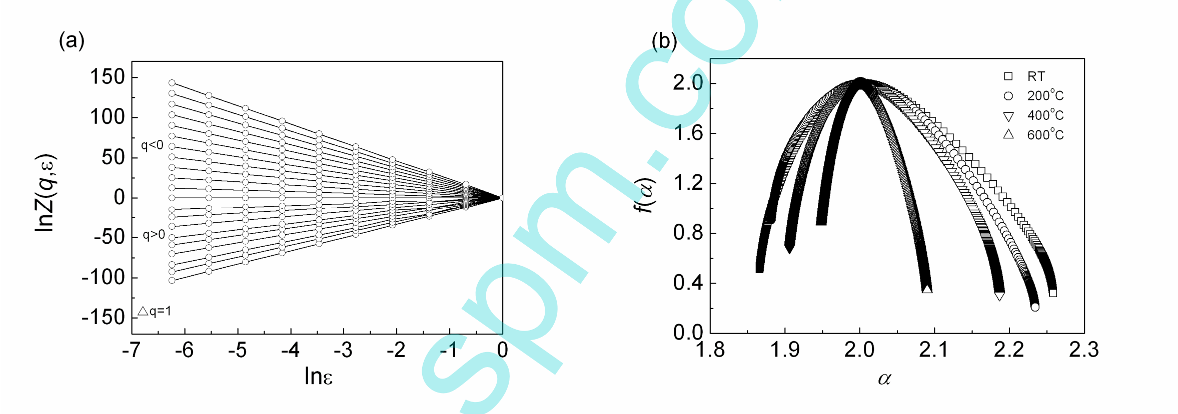

Fig.2 (a) $\ln Z(q,\varepsilon)$ -$\ln\varepsilon$ plots and (b) multifractal spectra of HfO_2 films

Table1. Influence of substrate temperature on structural and morphological characteristics

	Sample	RT	Substrate temp.200℃	Substrate temp.400℃	Substrate temp.600℃
XRD	2θ(-111)(degree)	28.16	28.23	28.28	28.08
	d_{-111}-spacing (Å)	3.169	3.161	3.156	3.178
	Grain size (nm)	4.2	5.1	6.8	14.8
AFM	R_a(nm)	3.78	3.59	2.06	0.67
	rms(nm)	4.88	4.82	2.66	0.84
	α_{max}	2.2586	2.2345	2.1867	2.090
	$f(\alpha_{max})$	0.3196	0.2086	0.3044	0.3457
	α_{min}	1.8663	1.8818	1.9062	1.9484
	$f(\alpha_{min})$	0.5112	0.9058	0.6823	0.8874
	$\Delta\alpha$	0.3923	0.3527	0.2805	0.1416
	Δf	+0.1916	+0.6972	+0.3779	+0.5417

Structural properties. The XRD patterns of HfO_2 films grown on Si (001) at various temperatures are shown in Fig.3 (a).

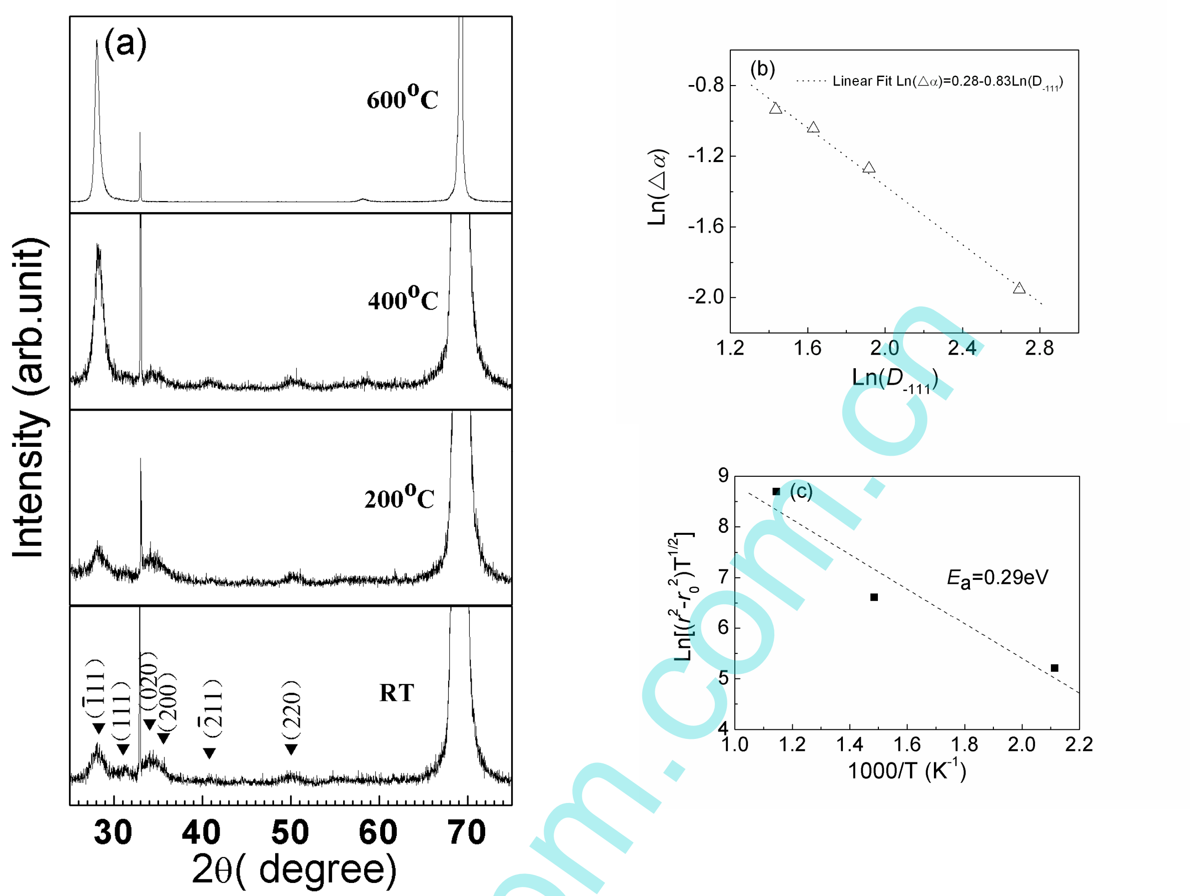

Fig.3 (a) XRD spectra of HfO_2 films as a function of temperature, (b) ln $\Delta\alpha$-ln $D_{(-111)}$ plots, (c) $\ln[(r^2-r_0^2)T^{1/2}]$-$1/T$ plots

The XRD curves of all HfO_2 films indicate the polycrystalline nature of samples. The peaks can be unambiguously assigned to monoclinic HfO_2 as labeled in Fig.3 (a) (referenced JCPDS 74-1506). For HfO_2 grown at RT ~ 200 °C, the peak at the 2θ angle of ~ 28.3° corresponds to (-111) orientation is seen to be very broad, indicating the presence of very small nanoparticles. It is evident that the x-ray peak intensity at 28.3°, which corresponds to diffraction from (-111) planes, increases with increasing substrate temperature. XRD curve of HfO_2 films grown at 600 °C indicates their well and highly oriented nature. This is an indicative of an increase in average crystalline size and preferred orientation along (-111). Crystallites with (-111) planes oriented perpendicular to the growth direction in a film therefore represent the lowest energy orientation and are thermodynamically preferred. The average grain size was estimated according to the Scherrer equation from the full width at half maximum (FWHM) of the -111 reflection peak, obtained by fitting the spectra by Gaussian shaped lines. The mean grain size $D_{(-111)}$ is 4.2 nm, 5.1 nm, 6.8 nm, and 14.8 nm for HfO_2 films grown at RT, 200 °C, 400 °C, and 600 °C, respectively. The grain sizes become larger with the increasing temperature. As listed in table1, it is important to recognize that d spacing (d_{-111}) decreases with increasing grain size below 7 nm, but becomes larger with grain size of 14.8 nm. The strain induced in the (-111) preferred orientation of the film may be the main reason for the lattice expansion with grain size of 14.8 nm. On the other hand, the lattice expansion in ionic solids with grain size of below10nm occurs either due to the reduction in cation charge state or repulsion of strong surface dipoles leading to a reduction in surface tension in small crystalline. Alta and Cisneros-Morales [16] have reported that the surface dipole repulsion is responsible for the observe lattice expansion in small crystallines, because of formation of Hf cations with only a single charge state +2. Our results on the lattice expansion in crystalline HfO_2 films with grain size of below 7 nm agree with their results although the growth conditions and film thickness are different.

Fig.3 (b) also shows the relationship of $\Delta\alpha$ and the grain size of HfO_2 films. It was found that the widths $\Delta\alpha$ ($\Delta\alpha = \alpha_{max} - \alpha_{min}$) are related to the mean grain size $D_{(-111)}$ as $\Delta\alpha \propto [D_{(-111)}]^{-0.83}$. This result indicates that the difference between the lowest and the highest growth probability of the surface is decreased with the increase in the mean grain size of thin film. This is due to the enhanced mobility of sputtered species of Hf impinging on the substrate as a result of an increase in substrate temperature, leading to a larger rate of atoms joining together and, hence, formation of crystalline films with uniform height probability.

Growth behavior during film deposition is related to surface diffusion of adatoms on the substrate. Similar to diffusion coefficient, the motion rate of grain boundary is given by [17]

$$V_B = \frac{d\sigma}{dt} \approx V_0 \exp(-\frac{\Delta E}{kT}) \tag{7}$$

where σ is the area of the grain and t is the film growth time. k is the Boltaman constant, T is the absolute temperature. V_0 is inversely proportional to k_B and $T^{1/2}$, ΔE is the activation energy. The formula (7) results in

$$r^2 - r_0^2 \approx \frac{D_0}{k\sqrt{T}} \exp(-\frac{\Delta E}{kT}) \tag{8}$$

where the values of r_0, r_1, r_2, r_3 are the mean grain size $D_{(-111)}$ of 4.2 nm, 5.1 nm, 6.8 nm, and 14.8 nm for HfO_2 films grown at RT, 200 °C, 400 °C, and 600 °C, respectively, and D_0 is a constant. If we assume that the grain size is directly related to the surface diffusion of sputter-deposited species on the substrate surface. We can determine the value of ΔE by fitting the variation of $\ln[(r^2-r_0^2)]T^{1/2}$ as a function of $1/T$ if the growth time is same. For thermal-activated process of sputter-grown nanocrystalline HfO_2 films, the Arrhenius plot for the XRD data are shown in Fig.3 (c). The data indeed fit to a linear relation. The activation energy for HfO_2 films grown at elevated temperatures ($T_s \geq 200$ °C) determined from the slope of the linear plot is 0.29 eV. This value is expected for crystalline films with the grain sizes obtained, but higher than that of HfO_2 films reported by Ramana et al. [18], when compared to the data of some of the crystalline metal-oxide thin films [19-20].

Optical characterizations. The optical transmittance T and R measurements were performed to determine the optical constants of the HfO_2 films with a spectrophotometer in the spectral range from 190 to 1100 nm. From the transmittance measurements it is observed that all the films exhibit a high transmittance (> 80%) in visible region at normal incidence (no showing here).The complex refractive index (n-ik) and film thicknesses were calculated from R and T following an inverse synthesis method.

In Fig.4 the variation of refractive index of films grown at various temperatures is depicted as a function of wavelength. It is clear that a continuous increase in the refractive index is observed with increasing substrate temperature. The variation in refractive index at wavelength 633 nm from 1.87 to 2.01 as a function of crystalline size is shown as inset in Fig.5. It is found that the refractive index n_{633} increases and film deposition rate decreases with the increase in crystalline size. The film refractive index is related to the film density. The film packing density, P, defined as the ratio of volume of the solid part of film to the total volume of the film, can be calculated from the expression:

$$n^2 = \frac{(1-P)n_v^4 + (1+P)n_v^2 n_B^2}{(1+P)n_v^2 + (1-P)n_B^2} \quad (10)$$

where n, n_B, and n_v are the refractive index values of HfO_2 film, the void in the film, and HfO_2 bulk material, respectively. This equation was derived from an expression of Bragg and Pippard model. The packing density calculated from the refractive index data of HfO_2 films at λ = 633 nm (with n_s = 2.1 for bulk material and n_v for dry voids) is 0.88, 0.90, 0.94, and 0.95, respectively. It is increased with substrate temperature from RT to 600 °C. The increase in refractive index at RT~600 °C appears to be due to the increase in the packing density, which in turn is a result of the increase in the mobility of atoms at elevated temperature.

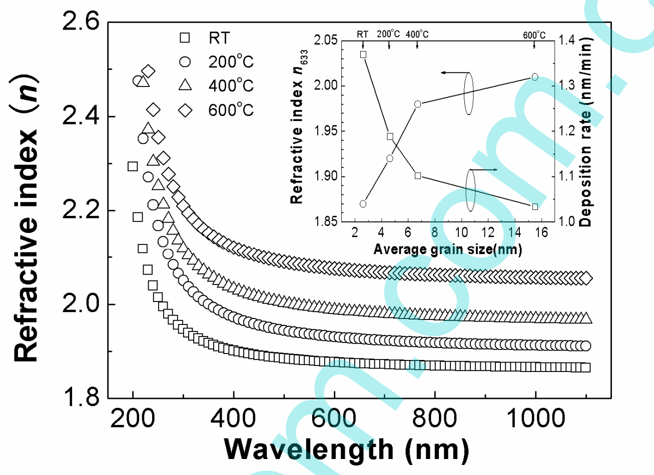

Fig.4 Refractive index of HfO_2 films grown at various temperatures, the inset is variation of refractive index n_{633} and deposition rate with grain size (or substrate temperature)

Conclusion

In summary, monoclinic HfO_2 films were grown by sputter deposition under varying substrate temperatures (T_s) and their multifractal, structural and optical properties were evaluated. The monoclinic HfO_2 is highly oriented along (-111) direction with increasing T_s. The film growth process at $T_s \geq$ 200 °C with surface diffusion energy of ~ 0.29 eV is evident from the structural analysis of HfO_2 films. Multifractal analysis shows the Δf of the multifractal spetra of the HfO_2 films is all bigger than zero and the uniformity of the height distribution increases as T_s is increased. The widths $\Delta\alpha$ of multifractal spectra depends on $D_{(-111)}$ as $[D_{(-111)}]^{-0.83}$ and the refractive index increases and the growth rate decreases with the increase in crystalline size.

Acknowledgements

The work is supported by Scientific Research Fund of Liaoning Provincial Education Department no.L2013476 and Fundamental Research Funds for the Central Universities no. DUT11LK44.

References

[1] C.D.Pemmaraju and S.Sanvito, Phys.Rev.Lett. 94 (2004) 217205.

[2] L.Armelo,H.Bertagnolli, D.Bleiner, M.Groenewolt, and S.Gross, Adv.Funct.Mater. 17 (2007)1671.

[3] G. D. Wilk, R. M. Wallace, and J. M. Anthony, J. Appl. Phys. 89 (2001) 52443.

[4] S.Sayan, S.Aravamudhan, B.W.Busch, W.H.Schulte, F.Cosandey, G.D,wilk, T.Gustafsson, and E.Garfunkel, J. Vac.Sci.Technol.A20 (2002) 507.

[5] T.Nishide, S.Honda, M.Matsuura, and M.Ide, Thin Solid Films 371 (2000) 61.

[6] S.J.Wang, P.C.Lim, A.C.H.Huan, C.L.Liu, J.W.Chai, S.Y.Chow, J.S.Pan, Q.Li, and C.K.Ong, Appl. Phys. Lett. 82 (2003) 2047.

[7] K.Cherkaoui, S.Monaghan, M.A.Negara, M.Modreanu, P.K.Hurley, D.O.Connell, S.McDonnell, G.Hughes, S.Wright, R.C.Barklie, P.Bailey, and T.C.Q.Noakes, J. Appl. Phys. 104 (2001) 064113

[8] S. Bruns, M. VergÖhl, O. Werner, and T. Wallendorf, Thin Solid Films 520(2012) 4122.

[9] B.B.Mandelbrot, Pure Appl.Geophys, 131(1989)5.

[10] R.Lopes and N.Betrouni, Med. Image Anal.13 (2009) 634.

[11] D.Labat, A.Mangin, and R.Ababou, J.Hydrol 256 (2002) 176.

[12] A. Chhabra and R.V.Jensen, Phys.Rev.Lett. 62(1989) 1327.

[13] A Chaudhari, C.C.S.Yan and S.L.Lee, Appl.Surf.Sci. 238(2004)513.

[14] D.Raoufi, H.R. Fallah, A Kiasatpour, and A.S.H.Rozatian Appl.Surf.Sci.254 (2008)2168.

[15] Z.W.Chen, X.P.Wang, S.Tan, S.Y.Zhang, J.G.Hou, and Z.Q.Wu, Phys.Rev.B63 (2001) 165413.

[16] Cisneros-Morales and M.C.Aita, Appl. Phys. Lett. 96 (2010) 191904.

[17] M Ohring, Materials Science of Thin Films, (Academic Press, San Diego 2002), pp.641.

[18] C.V.Ramana, K.Kamala. Bharathi, A.Garcia, and A.L.Campbell, J.Phys.Chem,C 116(2012)9955.

[19] S.K.Gullapalli, R.S.Vemuri, and C.V. Ramana, Appl. Phys. Lett. 96 (2010) 171903.

[20] H.J.Li, C.Y.Pu, C.Y.Ma, Sh.Li, W.J.Dong, S.Y.Bao, and Q.Y.Zhang, Thin Solid Films 520(2011) 212.

Current Research on Functional Materials
10.4028/www.scientific.net/AMR.1053

Multifractal, Structural and Optical Properties of HfO_2 Thin Films
10.4028/www.scientific.net/AMR.1053.343

DOI References

[1] C.D. Pemmaraju and S. Sanvito, Phys. Rev. Lett. 94 (2004) 217205.
http://dx.doi.org/10.1103/PhysRevLett.94.217205
[2] L. Armelo,H. Bertagnolli, D. Bleiner, M. Groenewolt, and S. Gross, Adv. Funct. Mater. 17 (2007)1671.
http://dx.doi.org/10.1002/adfm.200600458
[3] G. D. Wilk, R. M. Wallace, and J. M. Anthony, J. Appl. Phys. 89 (2001) 52443.
http://dx.doi.org/10.1063/1.1361065
[4] S. Sayan, S. Aravamudhan, B.W. Busch, W.H. Schulte, F. Cosandey, G. D, wilk, T. Gustafsson, and E. Garfunkel, J. Vac. Sci. Technol. A20 (2002) 507.
http://dx.doi.org/10.1116/1.1450584
[5] T. Nishide, S. Honda, M. Matsuura, and M. Ide, Thin Solid Films 371 (2000) 61.
http://dx.doi.org/10.1016/S0040-6090(00)01010-5
[7] K. Cherkaoui, S. Monaghan, M.A. Negara, M. Modreanu, P.K. Hurley, D.O. Connell, S. McDonnell, G. Hughes, S. Wright, R.C. Barklie, P. Bailey, and T.C.Q. Noakes, J. Appl. Phys. 104 (2001) 064113.
http://dx.doi.org/10.1063/1.2978209
[10] R. Lopes and N. Betrouni, Med. Image Anal. 13 (2009) 634.
http://dx.doi.org/10.1016/j.media.2009.05.003
[11] D. Labat, A. Mangin, and R. Ababou, J. Hydrol 256 (2002) 176.
http://dx.doi.org/10.1016/S0022-1694(01)00535-2
[14] D. Raoufi, H.R. Fallah, A Kiasatpour, and A.S.H. Rozatian Appl. Surf. Sci. 254 (2008)2168.
http://dx.doi.org/10.1016/j.apsusc.2007.09.015
[15] Z.W. Chen, X.P. Wang, S. Tan, S.Y. Zhang, J.G. Hou, and Z.Q. Wu, Phys. Rev. B63 (2001) 165413.
http://dx.doi.org/10.1103/PhysRevB.63.165413
[16] Cisneros-Morales and M.C. Aita, Appl. Phys. Lett. 96 (2010) 191904.
http://dx.doi.org/10.1063/1.3428965
[19] S.K. Gullapalli, R.S. Vemuri, and C.V. Ramana, Appl. Phys. Lett. 96 (2010) 171903.
http://dx.doi.org/10.1063/1.3421540